Phosphorylation of Connexin43 on Serine368 by Protein Kinase C Regulates Gap Junctional Communication

Paul D. Lampe,* Erica M. TenBroek,‡ Janis M. Burt,§ Wendy E. Kurata,‖ Ross G. Johnson,‡ and Alan F. Lau‖

*Fred Hutchinson Cancer Research Center, Seattle, Washington 98109; ‡Department of Genetics, Cell Biology and Development, University of Minnesota, St. Paul, Minnesota 55108; §Department of Physiology, University of Arizona, Tucson, Arizona 85724; and ‖Molecular Carcinogenesis Section, Cancer Research Center, University of Hawaii, Honolulu, Hawaii 96813

Abstract. Phorbol esters (e.g., TPA) activate protein kinase C (PKC), increase connexin43 (Cx43) phosphorylation, and decrease cell–cell communication via gap junctions in many cell types. We asked whether PKC directly phosphorylates and regulates Cx43. Rat epithelial T51B cells metabolically labeled with $^{32}P_i$ yielded two-dimensional phosphotryptic maps of Cx43 with several phosphopeptides that increased in intensity upon TPA treatment. One of these peptides comigrated with the major phosphopeptide observed after PKC phosphorylation of immunoaffinity-purified Cx43. Purification of this comigrating peptide and subsequent sequencing indicated that the phosphorylated serine was residue 368. To pursue the functional importance of phosphorylation at this site, fibroblasts from Cx43$^{-/-}$ mice were transfected with either wild-type (Cx43wt)

or mutant Cx43 (Cx43-S368A). Intercellular dye transfer studies revealed different responses to TPA and were followed by single channel analyses. TPA stimulation of T51B cells or Cx43wt-transfected fibroblasts caused a large increase in the relative frequency of ~50-pS channel events and a concomitant loss of ~100-pS channel events. This change to ~50-pS events was absent when cells transfected with Cx43-S368A were treated with TPA. These data strongly suggest that PKC directly phosphorylates Cx43 on S368 in vivo, which results in a change in single channel behavior that contributes to a decrease in intercellular communication.

Key words: gap junctions • connexins • tumor promoter • phosphorylation • carcinogenesis

Introduction

Gap junctions are specialized membrane domains composed of collections of channels that directly connect neighboring cells (Goodenough et al., 1996). These pathways provide for the cell-to-cell diffusion of small molecules, including ions, amino acids, nucleotides, and second messengers (e.g., calcium, cAMP, cGMP, and IP$_3$). By mediating the intercellular exchange of these and other signaling molecules, gap junctions are thought to affect cell growth control and embryonic development, as well as the transmission of electrical signals between cells. Recent studies on the targeted disruption of connexin genes, which encode gap junction channel proteins, provide strong support for these roles. Reduced control of cell growth with the deletion of connexin32 (Temme et al., 1997), the lack of essential developmental signaling with

loss of connexin37 (Simon et al., 1997) and altered electrical transmission in the heart in the absence of connexin40 (Simon et al., 1998) have been reported.

Given the importance of this communication system, the precise regulation of gap junction channels is considered critical for enabling signals to pass between cells at the appropriate time and place. The phosphorylation of connexins provides a key mechanism for regulating the gating of gap junction channels, as well as other aspects of connexin activity. Connexin43 (Cx43)[1] is phosphorylated at multiple serine residues in vivo (Crow et al., 1990; Musil et al., 1990; Brissette et al., 1991; Kadle et al., 1991; Laird et al., 1991; Berthoud et al., 1992; Cooper et al., 2000). The phosphorylation of Cx43 is not viewed as a requirement for the formation of functional channels, since truncated versions lacking the apparent phosphorylatable serines can form

[1]*Abbreviations used in this paper:* Cx43, connexin43; Cx43wt, wild-type connexin43; Cx43-S368A, S368A mutant Cx43; PKC, protein kinase C; TFA, trifluoroacetic acid; TPA, 12-*O*-tetradecanoylphorbol-13-acetate.

channels (Fishman et al., 1991; Dunham et al., 1992). Rather, the phosphorylation of gap junction proteins appears to regulate channel function and the rates of channel assembly and turnover (Brissette et al., 1991; Lampe, 1994; Kwak et al., 1995a,b,c).

Transient changes in junctional communication, probably regulated by signaling cascades, have been observed and appear necessary for normal cell cycling. However, in the sustained absence of such communication, tumorigenesis is enhanced (Laird et al., 1999; Moennikes et al., 1999). The correlation between neoplastic transformation and reduced gap junctional communication (Atkinson et al., 1981; Azarnia and Loewenstein, 1984; de Feijter et al., 1990) has led to the hypothesis that reduced cell–cell communication is a critical step in multistage carcinogenesis (Fitzgerald and Yamasaki, 1990; Trosko et al., 1990).

Protein kinase C (PKC) has received considerable attention because PKC activators (e.g., 12-*O*-tetradecanoylphorbol-13-acetate (TPA); see Nishizuka, 1986), which promote tumorigenesis, both increase Cx43 phosphorylation and decrease gap junction communication in a number of different cell types (Brissette et al., 1991; Berthoud et al., 1992, 1993; Reynhout et al., 1992; Lampe, 1994). The action of phorbol esters on gap junction communication has been reported to involve inhibition of junction assembly and modification of channel properties (Lampe, 1994; Kwak et al., 1995a,c). Whether PKC acts directly on Cx43 protein in vivo and, if so, how this modification specifically affects function at the level of individual GJ channels has not been elucidated. We report here that S368 is a major site of PKC phosphorylation in Cx43. Using cells transfected with Cx43wt or Cx43-S368A, this site is shown to underlie the TPA-induced reduction in intercellular communication and alteration of single channel behavior. This molecular precision helps explain the actions of TPA and PKC in depressing gap junction communication and provides insight into the poorly understood role of TPA as a tumor promoter.

Materials and Methods

Cx43$^{-/-}$ Cell Line Maintenance and Transfection

The Cx43$^{-/-}$ mouse cell line $^{-/-}$3 (Martyn et al., 1997) and transfectants were propagated in DME with 10 mM Hepes (Life Technologies, Inc.) containing 10% fetal calf serum (Hyclone) and penicillin/streptomycin in a humidified 5% CO$_2$ incubator at 37°C as described (Martyn et al., 1997). The $^{-/-}$3 fibroblasts were transfected with wild-type rat Cx43 cDNA (Beyer et al., 1987) excised from pBluescript with EcoR1 and BamH1 and inserted into pZeoSV (Invitrogen). Stably transfected wild-type Cx43 fibroblast clones 22C-3 (also known as 3R1; Martyn et al., 1997) and 25C-2 were isolated by repeated dilution subcloning in the selective antibiotic zeocin (350 μg/ml). Serine to alanine site 368 mutant Cx43 cDNA was generated using the Chameleon double-stranded, site-directed mutagenesis kit (Stratagene) and was then subcloned into the bicistronic expression vector pIREShyg (Clonetech) and transfected into the $^{-/-}$3 cell line. Stably transfected clones pI8 and pI9 were isolated by repeated dilution subcloning using progressively higher concentrations of the selective antibiotic hygromycin (75–500 μg/ml). Clones were established and maintained in 100 μg/ml ECGS (Becton Dickinson).

Metabolic Labeling and Cx43 Immunoprecipitation

T51B rat liver epithelial and Cx43$^{-/-}$ transfectants (clones 22C-3 and pI8) were cultured, metabolically labeled with $^{32}P_i$, and immunoprecipitated as previously described (Kanemitsu and Lau, 1993). In brief, cells were la-

beled with $^{32}P_i$ (NEX-053; NEN Life Science Products) at 3.0 mCi/ml for 3 h in phosphate-deficient medium (GIBCO BRL) and, where indicated, were treated with 100 ng/ml TPA during the final 30 min. The cells were rinsed in PBS, lysed in RIPA buffer (150 mM NaCl, 1% sodium deoxycholate, 1% Triton X-100, 0.1% SDS, 10 mM Tris-HCl, pH 7.2), clarified, and immunoprecipitated with Cx43-CT368 peptide antiserum or nonimmune serum.

Two-dimensional Phosphoamino Acid Analysis

Two-dimensional phosphoamino acid analysis was performed as previously described (Loo et al., 1995). The immunoprecipitated, SDS-PAGE–purified samples were blotted to Immobilon-P membrane, the band corresponding to Cx43 was excised, the membrane was acid hydrolyzed, and the released amino acids were lyophilized and mixed with unlabeled phosphoserine, phosphothreonine, and phosphotyrosine standards. The samples were electrophoresed on thin layer cellulose sheets in pH 1.9 buffer in the first dimension and then in pH 3.5 buffer in the second dimension (Kamps and Sefton, 1989). Standards were visualized by ninhydrin staining and the sheets were exposed to Kodak X-OMAT XAR-5 film with an intensifying screen for 2–4 d at −70°C. Densitometry of autoradiographs was performed on a Macintosh G3 using a Hewlett Packard Scan-Jet 3c to collect the image and the public domain NIH Image program (developed at the U.S. National Institutes of Health and available at http://rsb.info.nih.gov/nih-image/).

Expression and Purification of Cx43

Full-length Cx43 was expressed in Sf9 insect cells infected with a recombinant baculovirus containing the rat Cx43 cDNA (Loo et al., 1995). Cx43 was isolated from membrane pellets of Sf9 cell homogenates by detergent extraction and was immunoaffinity purified by incubation with a protein G–Sepharose cross-linked monoclonal antibody to Cx43.

In Vitro Phosphorylation with PKC

PKC was purified from bovine brain by a method described previously (Bazzi and Nelsestuen, 1987). The PKC preparations used in this study (a mixture of α-, β-, and γ-isozymes) showed high activity and strong dependence on calcium, diacylglycerol, and phospholipids when tested with histone as the substrate (Bazzi and Nelsestuen, 1992). Mixed micelles containing 20 mol% phosphatidylserine were prepared by evaporating organic solvents and suspending the phospholipid directly in 0.5 ml of buffer containing 20 mM Tris-HCl, pH 7.8, 2% (wt/wt) Triton X-100 (Hannun et al., 1985). Purified, full-length Cx43 (solubilized in 1% Triton X-100) was phosphorylated by PKC in mixed micelles (100 μM phosphatidylserine) with 15 mM MgCl$_2$, 2 mM CaCl$_2$, 200 nM TPA, 40 μM γ-[^{32}P]-ATP (Amersham PB170, 3 Ci/mmol), 10 mM Tris-HCl (pH 8.0), and Triton X-100 (0.2% final concentration). For phosphorylation of Cx43-derived peptide D360-I382, phosphatidylserine/phosphatidylcholine (40/60 mol%) vesicles were prepared by sonication of dried phospholipids (0.5 mg/ml) in buffer (20 mM Tris, pH 8.0 containing 100 mM NaCl). Final concentrations in these reactions were 0.25 mg/ml phospholipid, 10 mM MgCl$_2$, 2 mM CaCl$_2$, 200 nM TPA, 40 μM γ-[^{32}P]-ATP (Amersham PB170, 3 Ci/mmol), and 10 mM Tris-HCl (pH 8.0). The reactions were initiated by the simultaneous addition of the ATP and MgCl$_2$. After proceeding for 30–60 min, the reactions were terminated by the addition of Laemmli sample buffer for the full-length Cx43 or injected into the HPLC for peptide D360-I382. Cx43 purified from baculovirus and Cx43 immunoprecipitated from T51B epithelial cells were separated on 10.0 or 12.5% polyacrylamide gels following published methods (Laemmli, 1970).

Trypsin Digestion and Two-dimensional Phosphotryptic Peptide Analysis

After SDS-PAGE, the Cx43 protein band was identified by autoradiography of the unfixed, wet gel using Kodak X-OMAT film. Phosphorylated Cx43 was extracted from the gel pieces and precipitated on ice with trichloroacetic acid. The precipitated protein was digested overnight with 0.4 μg sequencing grade trypsin (Promega). The phosphotryptic peptides were either separated by HPLC or were resolved on cellulose thin-layer chromatography plates (EM Science) by electrophoresis in the first dimension and chromatography in the second as described previously (Kanemitsu and Lau, 1993).

High Performance Liquid Chromatography

High performance liquid chromatography (HPLC) separation of peptides was performed on a Hewlett Packard 1050 LC using a BioRad Microsorb C18 reverse phase column (5 μm, 300 Å) at 37°C. A linear gradient from 99.9:0:0.1 water/acetonitrile/trifluoroacetic acid to 59.9:40:0.1 over 40 min was used, followed by an increase to 99.9% acetonitrile in 5 min. Fractions were taken every min and they were counted without fluor in a Beckman scintillation counter.

Peptide Sequencing

HPLC-purified fraction 8 and peptide D360-I382 were sequenced on an automated protein sequencer (Applied Biosystems Division Model 477A; Perkin Elmer) using pulsed liquid chemistry. Phenylthiohydantoin amino acids were analyzed on a phenylthiohydantoin amino acid analyzer (Applied Biosystems Division Model 120A; Perkin Elmer) using ultraviolet detection. Standard reagents and conditions were employed. Peptide D360-I382 was sequenced and was shown to correspond to the last 23 amino acids of the rat Cx43 sequence with an additional cysteine residue on the NH_2-terminal end originally added for cross-linking and antibody production purposes.

For determination of the position of the phosphorylated residue, phosphorylated D360-I382 peptide and fraction 8 from in vivo phosphorylated material were covalently bound via carboxyl groups to Sequelon-AA (aryl-amine) disks (Millipore) using water soluble carbodiimide (Sullivan and Wong, 1991). The standard sequencing protocol was modified with direct collection of neat TFA extraction steps in each cycle to thoroughly wash off any noncovalently bound phosphorylated residues and $^{32}P_i$ (Russo et al., 1992). Fractions were then counted in a Beckman Model 3801 scintillation counter. To maintain alignment with the actual Cx43 sequence, the sequencing $^{32}P_i$ release value for the N-terminal cysteine (580 cpm) of peptide 360–382 was omitted from the histogram and the cycle numbers presented are one cycle less than the actual number performed.

Dye Coupling and Electrophysiology

To evaluate gap junctional permeability, Lucifer yellow CH (4.0%) was introduced into pI8, pI9, or 22C-3 clones using a 5-s pulse of hyperpolarizing current (1.1 nAmp). The number of injections resulting in dye transfer (incidence of dye coupling) and the number of cells receiving dye when coupled (extent of dye coupling) were assessed 3 min after microinjection using a Zeiss IM35 fluorescence microscope equipped with a DVC digital camera and Image Pro 4.0 capture software. For examination of the effect of TPA on gap junctional communication, pI8 or 22C-3 cells were first trypsinized and reaggregated as confluent monolayers at 37°C for 4–6 h. Cells were then removed from the incubator, allowed to reach room temperature, and then treated with TPA (0 or 50 ng/ml) for 0–120 min before evaluation of permeability.

For single channel studies, confluent cells were trypsinized and replated at low density on glass coverslips for examination of the coupling between cell pairs. After 3–4 h at 37°C, the cells were treated with TPA (0 or 50 ng/ml in culture medium) at room temperature for 60–140 min in the presence of 5% CO_2 before data acquisition. During recording sessions, the cells were bathed in solution containing: 142.5 mM NaCl, 4 mM KCl, 1 mM $MgCl_2$, 5 mM glucose, 2 mM sodium pyruvate, 10 mM Hepes, 1 mM $BaCl_2$, 1 mM $CaCl_2$, 15 mM CsCl, and 10 mM TEACl, pH 7.2, and osmolarity 315 mOsM. The pipet solution contained: 120 mM KCl, 14 mM CsCl, 3 mM $MgCl_2$, 5 mM glucose, 9 mM Hepes, 9 mM EGTA, 9 mM TEACl, 5 mM Na_2ATP, 30 mM KOH, pH 7.2, and 315 mOsM. Single channel events were visualized using a dual whole-cell voltage clamp as described previously (He et al., 1999). Transjunctional driving force was 40 mV in all experiments and cells were superfused with 4 mM halothane (Burt and Spray, 1989) to reduce junctional conductance to levels where single channel events could be observed. Junctional current was digitized and acquired for analysis (Ramanan and Brink, 1993) and display. For construction of event amplitude-relative frequency histograms, the amplitudes of channel events were measured by hand and sorted into 6.25-pS bins (e.g., 25–31.25, 31.26–37.5, and 37.51–43.75 pS, etc.). The frequency of the event amplitudes within a bin was calculated as a function of the total number of events in the treatment group and plotted.

Results

Cx43 Phosphorylation Is Increased In Vivo by TPA Treatment

As has been shown previously in other cell types, T51B rat liver epithelial cells that were metabolically labeled with $^{32}P_i$ yielded multiple, phosphorylated protein bands in the 43–47-kD range when immunoprecipitated with Cx43 antibody (Fig. 1 A, CON lane). Note that upon phosphorylation, the mobility of Cx43 in SDS-PAGE decreases and immunoprecipitation of Cx43 usually yields multiple bands that represent different phosphorylation states (Musil et al., 1990). If TPA was added during the last 30 min of the 3-h radiolabeling period, the phosphorylation of Cx43 increased dramatically (approximately fivefold, Fig. 1 A, TPA lane). Phosphoamino acid analysis of Cx43 immunoprecipitated from both the basal and TPA-treated cells yielded only phosphoserine (Fig. 1 B).

Phosphorylation of Cx43 In Vitro by PKC and Phosphotryptic Analysis

Phosphotryptic peptide analysis was used to examine the PKC-phosphorylated sites in Cx43 (Fig. 2). Cx43 isolated from untreated or TPA-treated T51B epithelial cells showed several phosphorylated peptides (Fig. 2, A and B). TPA treatment reproducibly stimulated the phosphorylation of several Cx43 peptides (three are indicated by brackets), whereas other peptides remained phosphorylated to the same extent or may have even been reduced. The intensity of one peptide (marked by arrows) was increased approximately fivefold relative to the phosphopeptide marked with an asterisk in Fig. 2, A and B.

Immunoaffinity-purified Cx43 was phosphorylated efficiently by PKC in an in vitro assay that used a Triton X-100/phosphatidylserine mixed micelle system (Hannun et al., 1985; Fig. 1 C). Two-dimensional phosphotryptic
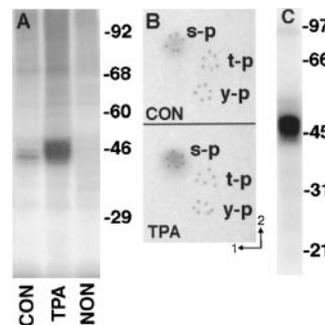

Figure 1. Phosphorylation of Cx43. (A) Cx43 was immunoprecipitated from control (CON) and TPA-treated (TPA) T51B rat liver epithelial cells metabolically labeled with $^{32}P_i$ at 0.5 mCi/ml for 3 h. TPA (100 ng/ml) was added 30 min before the end of the labeling period where indicated. Immunoprecipitates were prepared using either nonimmune (NON) or Cx43 CT368 peptide antiserum (CON & TPA) and resolved by SDS-PAGE. (B) Phosphoamino acid analysis of ^{32}P-labeled Cx43 purified from T51B cells, hydrolyzed and resolved by two-dimensional electrophoresis. Arrows indicate the direction of the electrophoresis in the first (pH 1.9) and the second (pH 3.5) dimension. Positions of unlabeled ninhydrin-stained phosphoamino acid standards are outlined: phosphoserine (s-p), phosphothreonine (t-p) and phosphotyrosine (y-p). C, PKC phosphorylation of immunoaffinity-purified Cx43. Cx43 was purified and phosphorylated with PKC in vitro as indicated in Materials and Methods. The sample was resolved by SDS-PAGE, and the wet gel was subjected to autoradiography for 3.5 h.

A. T51B | **B. T51B/TPA**
C. Cx43/PKC | **D. D360-I382/PKC**
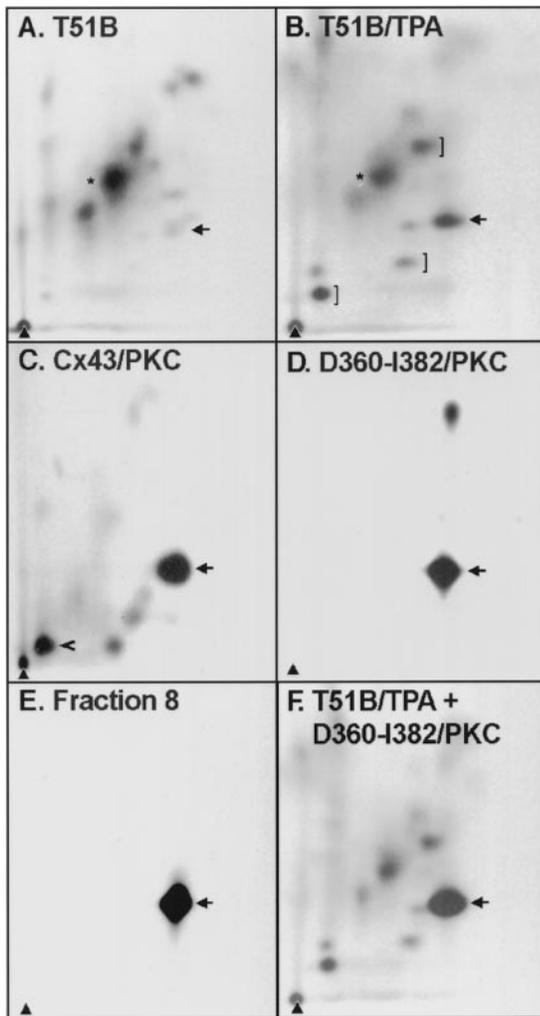**E. Fraction 8** | **F. T51B/TPA + D360-I382/PKC**

Figure 2. Two-dimensional phosphotryptic analysis of Cx43 and Cx43-derived peptides. Cx43 metabolically labeled and immunoprecipitated from T51B cells either untreated (A) or treated (B) with TPA. (C) Immunopurified and PKC-phosphorylated Cx43. (D) Peptide 360-382 of Cx43 phosphorylated by PKC. E, HPLC 8-min fraction from PKC-phosphorylated and trypsinized peptide 360-382. (F) Mixture of samples shown in B and E.

peptide analysis of full-length Cx43 phosphorylated in vitro by PKC indicated that the main phosphoacceptor (Fig. 2 C, arrow) comigrated with the major TPA-induced phosphopeptide (compare Fig. 2, B with C). Furthermore, PKC phosphorylated the same peptide when a gluta-thione-*S*-transferase fusion protein with the COOH-terminal portion (amino acids 236–382) of Cx43 was used as a substrate (data not shown). PKC also phosphorylated a peptide (marked with an arrowhead in C) in full-length Cx43 that may correspond to one of the phosphopeptides marked with brackets in Fig. 2 B. However, this peptide was not phosphorylated significantly when the fusion protein containing amino acids 236–382 was phosphorylated by PKC and, thus, could not be readily identified.

To further refine the site of PKC phosphorylation in the COOH-terminal tail of Cx43, a synthetic Cx43 peptide corresponding to residues D360-I382 was phosphorylated

by PKC in vitro. This peptide contains overlapping RX-SSR repeats that have been suggested as potential PKC and protein kinase A phosphorylation sites (Stagg and Fletcher, 1990). Tryptic peptide analysis of the PKC-phosphorylated Cx43 peptide revealed two phosphorylated spots (Fig. 2 D). The major phosphopeptide (Fig. 2 D, arrow) comigrated with the major in vivo TPA-responsive peptide and the major in vitro peptide phosphorylated by PKC in full-length Cx43 (compare Fig. 2, D with B and C). These data suggest that purified PKC recognized and phosphorylated the same site(s) in the COOH-terminal 23 amino acids of Cx43 that is induced by TPA in intact cells.

Identification of an In Vitro Cx43 PKC Phosphorylation Site

To identify the phosphoserine site(s) contained in the major in vitro Cx43-phosphorylated peptide, we used a combination of techniques including HPLC, two-dimensional tryptic peptide mapping, protein sequencing, and Edman degradation. Tryptic phosphopeptides of PKC-phosphorylated D360-I382 were resolved by reverse phase HPLC. A major peak that eluted at 8 min was observed in the HPLC profile (Fig. 3 A). This 8-min peak comigrated with a minor peak resolved from Cx43 isolated from TPA-treated cells (Fig. 3 B). Two-dimensional tryptic peptide analysis of the fractions revealed that the 8-min peak contained a single phosphopeptide (Fig. 2 E) that corresponded to the phosphopeptide indicated in Fig. 2 D by the arrow (peptide mix data not shown). Most importantly, the 8-min peak phosphopeptide clearly comigrated with the major Cx43 peptide whose phosphorylation was stimulated by TPA in intact cells (Fig. 2 F, arrow; compare with A and B).

Sequencing of the ^{32}P-labeled peptide that purified at 8 min yielded ASSR. This sequence is consistent with the first 4 residues of either tryptic peptide A367-R370 (ASSR) or A371-I382 (ASSRPRPDDLEI), both of which are in the terminal 16 amino acids of Cx43. Because there was no evidence of a proline residue at cycle 5, tryptic peptide A367-R370 was most likely present in the 8-min peak.

Since the A367-R370 and A371-I382 tryptic peptides are both contained in the synthetic D360-I382 peptide that was phosphorylated by PKC to yield the phosphopeptide of interest (Fig. 2 D), we used the D360-I382 peptide to positively identify the PKC phosphorylation site(s). We
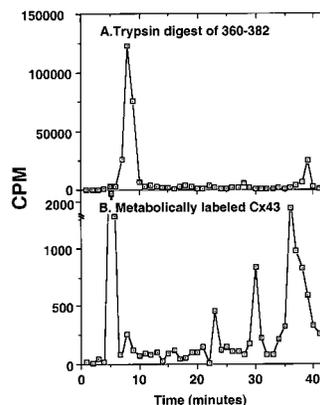

Figure 3. HPLC of PKC-phosphorylated fragments of Cx43. (A) Peptide 360-382 was phosphorylated by PKC, purified by HPLC, with trypsin, and repurified by HPLC. The smaller peak at 39 min represents undigested 360-382. (B) Cx43 from ^{32}P$_i$, metabolically labeled, TPA-treated T51B cells was trypsinized and separated via reverse phase HPLC.
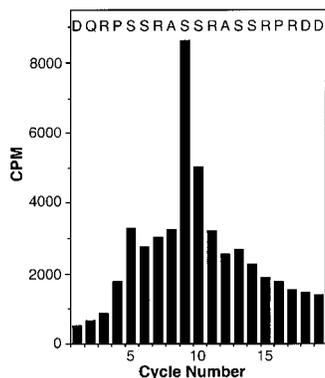
Figure 4. Identification of the phosphorylated residues in peptide 360-382. The number of cpm released during each cycle of Edman degradation is shown for the corresponding residue in the sequence. Cycle 9 which corresponds to S368 had the highest release of ^{32}P.

covalently linked the in vitro PKC-phosphorylated D360-I382 peptide to Sequelon membrane and performed Edman degradation to determine the cycle in which ^{32}P radioactivity was released. A major peak of ^{32}P radioactivity was observed at cycle 9 which corresponded to S368 of Cx43 (Fig. 4). Although cycle 10, which corresponds to S369, contains the second highest level of ^{32}P, this probably does not correspond to actual phosphorylation at 369; rather, it is probably indicative of incomplete conversion and cleavage during Edman degradation. With an assumption of 95% yields, iterative calculations show that after 9 cycles, 60% of the peptide left in the sequencer would be 14 amino acids long (the proper length), 31% of the peptide would be 15 amino acids long, and 9% 16 or longer. Similar calculations indicate that phosphorylation at S364 (cycle 5) was <20% of the phosphorylation at S368. Release of some ^{32}P a cycle or so before (preview) and several cycles after (lag) a phosphorylated residue has been shown for several other proteins (Shannon and Fox, 1995).

These data did not exclude the possibility that S369 was the actual in vivo phosphorylation site in this peptide instead of S368. To resolve this uncertainty, we immunoprecipitated metabolically phosphorylated Cx43 from TPA-treated T51B cells, purified Cx43 via SDS-PAGE, digested Cx43 with trypsin, and separated the tryptic fragments by reverse phase HPLC. Several peaks of radioactivity were observed (Fig. 3 B). The 5-min peak consisted mostly of free phosphate that did not bind to the column. The small peak at the 8-min elution time point was the only one in common with the eluted peaks from synthetic peptide D360-I382 (Fig. 3 A). Material in this 8-min peak was covalently linked to Sequelon membrane and subjected to Edman degradation. Although this sample contained a lower level of ^{32}P radioactivity because it originated from in vivo labeling conditions, cycle 2 of the Edman procedure (corresponding to S368) contained the highest level of radioactivity (cycle 1, 54 cpm; cycle 2, 208 cpm; cycle 3, 105 cpm; cycle 4, 111 cpm). These results supported the conclusion that phosphorylation of S368 in Cx43 is stimulated by TPA treatment of cells.

Site-directed Mutagenesis of S368 and Gap Junctional Communication

To determine whether S368 was necessary for TPA-induced reduction of cell–cell coupling, we used site directed mutagenesis to convert the serine into a non-phosphorylat-

able alanine residue and transfected fibroblasts prepared from Cx43$^{-/-}$ mice (Martyn et al., 1997) with either wild-type Cx43 (Cx43wt) or the S368A mutant Cx43 (Cx43-S368A). We then determined the incidence and extent of dye coupling between Cx43wt- and Cx43-S368A–transfected cells after treatment with either 0 or 50 ng/ml TPA (see Table I). In Cx43wt-transfected cells (22C-3 clone), the extent of Lucifer yellow dye coupling decreased to 54 and 12% of initial levels following 60 or 120 min of TPA treatment, respectively. In contrast, the extent of dye coupling in the Cx43-S368A cells (pI8 clone) only decreased to 97 and 87% of initial levels after 60 and 120 min. In addition, the incidence of coupling was totally unaffected by TPA treatment. Thus, the effects of TPA treatment on dye permeability between Cx43wt and pI8 cells were very different. We proceeded to evaluate the effect of TPA on dye transfer in another S368A clone (pI9), where we found no effect on the extent of transfer for up to 60 min in TPA. However, the incidence of coupling in this clone was decreased significantly after 60 min of TPA treatment (see Discussion). Concurrently with the pI9 dye studies, electrophysiological studies were initiated, since we reasoned that the varying responses of wild-type and mutant-transfected cells to TPA might reflect differences in single channel behavior. Phosphorylation of Cx43 has been reported to alter the unitary behavior of Cx43 (Moreno et al., 1994), although other alterations of gating behavior might also occur. To determine whether any TPA-induced changes in the single channel behavior of Cx43wt might be eliminated in the Cx43-S368A mutant, we examined single channel events under control and TPA treatment conditions in Cx43wt- and Cx43-S368A–transfected cells and in T51B cells.

Representative single channel records obtained from Cx43wt-transfected cells under control conditions and during TPA treatment are illustrated in Fig. 5. Note that events of ~100-pS amplitude predominated under control conditions (Fig. 5 A), whereas ~50-pS events predominated following 60–140 min of TPA treatment (Fig. 5 B). The amplitudes of more than 600 events from control and TPA-treated Cx43wt-transfected cells were measured, and

Table I. Analysis of Dye Transfer

Time in TPA		Average no. of cells receiving dye ± SEM*	Incidence of coupling‡
Cx43wt (22C-3)	Control (0)	9.0 ± 1.1	95.5% ($n = 22$)
	30–40 min	8.4 ± 1.3	93.3% ($n = 15$)
	60 min	4.9 ± 0.6	84.2% ($n = 19$)
	120 min	1.1 ± 0.3	64.7% ($n = 17$)
S368A (pI8)	Control (0)	20.5 ± 3.7	100% ($n = 6$)
	30–40 min	16.8 ± 2.6	100% ($n = 10$)
	60 min	20.0 ± 2.7	100% ($n = 10$)
	120 min	17.8 ± 2.6	100% ($n = 12$)
S368A (pI9)	Control (0)	4.2 ± 0.9	67.0% ($n = 10$)
	30–40 min	5.0 ± 1.6	22.2% ($n = 18$)
	60 min	5.2 ± 1.7	26.0% ($n = 19$)
	120 min	1.0 ± 0.0	25.0% ($n = 16$)

*Excludes no transfers.
‡Number of injections resulting in transfer/total number of injections, n = total number of injections.

A - Cx43wt - Control

77 pS   22 pS

99 pS   115 pS

B - Cx43wt - TPA

34 pS   47 pS   45 pS

53 pS

C - Cx43-S368A - Control

108 pS   93 pS   104 pS

48 pS   103 pS

110 pS   92 pS

D - Cx43-S368A - TPA

117 pS   95 pS

56 pS

110 pS
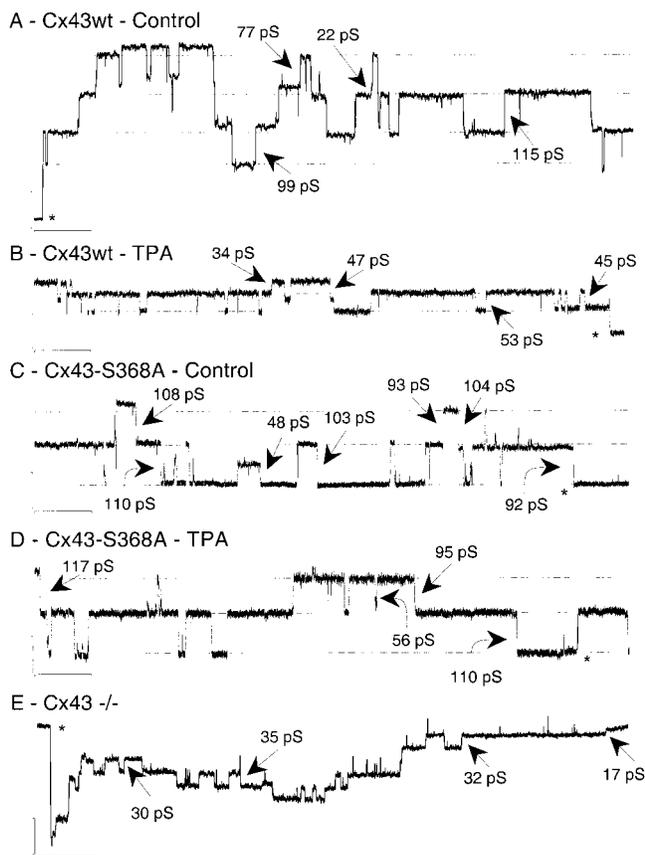
E - Cx43 -/-

35 pS

32 pS   17 pS

30 pS

Figure 5. TPA caused a decrease in event amplitude of Cx43wt but not Cx43-S368A channels. Under control conditions (A and C), ∼100-pS events predominate in wild-type–transfected (A) and S368A-transfected (C) cells. However, in the presence of TPA (B&D), ∼50-pS events predominate in the wild-type trans-fected cells (B), whereas the S368A-transfected cells continue to display ∼100-pS channels (D). Note the rapid voltage-dependent closure of Cx45 channels in Cx43$^{-/-}$ cells and the small channel amplitudes (E) compared with Cx43-transfected cells. Scale bars: vertical = 4pA, horizontal = 2 s. Transjunctional voltage was 40 mV in all records. Zero current in each trace is marked with an asterisk.

Figure 6. Event amplitude-relative frequency histograms of sin-gle channel data. The relative frequency of 87–112-pS channels was decreased in TPA-treated Cx43wt-transfected (A) but not Cx43-S368A–transfected (B) cells. Similarly, the relative fre-quency of the 50–68-pS channels was enhanced in TPA-treated Cx43wt- but not Cx43-S368A–transfected cells. The data were compiled from two independent clones of the wild-type (22C-3 and 25C-2) and the S368A (pI8 and pI9) transfectants. (C) T51B cells, which express Cx43wt, also displayed a decreased relative frequency of the 87–115-pS channels and increased relative fre-quency of 50–62-pS channels in response to TPA. (D) Cx43$^{-/-}$ cells, which express Cx45, exhibited predominantly 25–37.5-pS channels. (Cx43wt controls: 7 cell pairs, 648 events; Cx43wt TPA: 6 pairs, 742 events; Cx43-S368A controls: 8 pairs, 813 events; Cx43-S368A TPA: 7 pairs, 641 events, T51B controls: 2 pairs, 247 events; T51B TPA: 4 pairs, 102 events; Cx43$^{-/-}$ cells: 5 pairs, 219 events).

the relative frequency of each event amplitude was plotted in an event amplitude-relative frequency histogram (Fig. 6 A). Note that under control conditions 76% of all events had amplitudes between 87 and 112 pS, whereas following TPA treatment only 12% of events had amplitudes in this range. In contrast, the 50-pS population of channels (50–68 pS) comprised only 8% of all events under control conditions but totaled 63% after TPA treatment. Thus, TPA enhanced the relative frequency of the 50-pS events while simultaneously decreasing the relative frequency of the 100-pS events. Comparable results were observed in T51B rat epithelial cells (Fig. 6 C) wherein the 100-pS channel population comprised 66% of the total events un-der control conditions vs. 14% when treated with TPA and the 50-pS channel population comprised 25 vs. 52%, with-out and with TPA, respectively. Thus, the data from both the Cx43wt-transfected fibroblasts and the T51B rat epi-thelial cells indicated that TPA induced a reduction in rel-
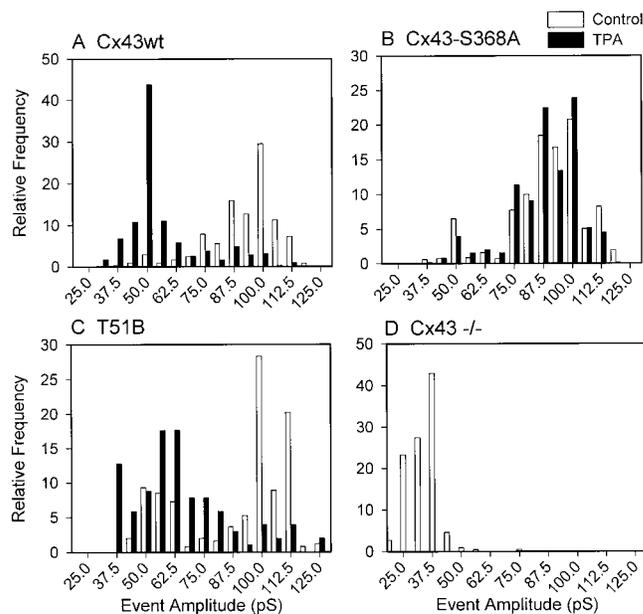
ative frequency of the 100-pS channel population and an increase in relative frequency of the 50-pS population.

Representative single channel records obtained from Cx43-S368A–transfected cells under control and TPA treatment conditions are illustrated in Fig. 5, C and D, re-spectively. Note that under both conditions, events of ∼100-pS amplitude predominated. The event amplitude-relative frequency histogram generated from >600 events measured in control and TPA-treated cells (Fig. 6 B) re-vealed that the 87–112-pS population comprised 69% of all events under both control and TPA treatment condi-tions, whereas the 50–68-pS population comprised only 9–10% of all events in both conditions and for both the pI8 and pI9 clones. Thus, it appears that mutation of S368 eliminated both the TPA-induced decrease in relative fre-quency of the 100-pS population of channels and the TPA-induced increase in relative frequency of the 50-pS popu-lation observed in the wild-type expressing cells.

Untransfected Cx43$^{-/-}$ cells express low levels of Cx45 (Martyn et al., 1997). The single channel events observed in these cells are unlike those observed in either the Cx43wt- or Cx43-S368A–transfected cells. Junctions in

Cx43$^{-/-}$ cells display significant voltage-dependent gating behavior (Fig. 5 E) that quickly renders the channels silent. Given the long duration pulses used in the experiments discussed above, these endogenous channels would not be expected to be readily evident in the records. In addition, the event amplitudes commonly observed in the Cx43wt and S368A cells were rarely observed in the Cx43$^{-/-}$ cells (Fig. 6 D). Indeed, only 1.4% of the total Cx45 channel events had amplitudes between 50 and 68 pS, and there were no events with amplitudes between 87 and 112 pS. The absence of events with diverse amplitudes (a hallmark feature of junctions containing heteromeric channels; He et al., 1999; Valiunas et al., 2000) in the Cx43wt and S368A cells also supports the conclusion that homomeric, heteromeric and heterotypic channels containing Cx45 comprise a negligible percentage of the total channel population as is consistent with the low level of Cx45 expression.

Phosphotryptic Peptide Analysis of Cx43wt- and Cx43-S368A–transfected Cx43$^{-/-}$ Cells

To confirm that Cx43wt-transfected Cx43$^{-/-}$ fibroblasts, like T51B cells, react to TPA with an increase in phosphorylation at S368, Cx43 was isolated from metabolically labeled Cx43wt (22C-3 clone)- and Cx43-S368A (pI8 clone)–transfected fibroblasts and subjected to two-dimensional phosphotryptic analysis (Fig. 7). Because the transfected Cx43$^{-/-}$ fibroblasts contain several-fold less phosphorylated Cx43 than the T51B cells, multiple week exposures were required and Cx43 had to be essentially overloaded onto the chromatography plates, which caused the central area of the map to be less well defined. However, the region where the S368-containing peptide migrated was well separated and defined. TPA stimulated the phosphorylation of a peptide (marked with an arrow) in Cx43wt-transfected cells that migrated in the region where the peptide containing S368 was found previously (compare Fig. 7, A and B with Fig. 2). Confirmation that this peptide contained S368 was obtained by examining the comigration of PKC phosphorylated, trypsin-digested D360-I382 (Fig. 7 C). Complete comigration of the phosphorylated A367-R370 peptide (C) with the peptide marked with an arrow in the TPA-treated Cx43wt transfectant (B) was demonstrated in the mix analysis (Fig. 7 D). As expected, this phosphopeptide was not present in Cx43-S368A–transfected cells that were untreated (not shown) or treated TPA with (Fig. 7 E) as shown by the mix with PKC-phosphorylated A367-R370 (Fig. 7 F). These data confirm that TPA treatment increased the phosphorylation of Cx43 at S368 site in the Cx43wt-transfected Cx43$^{-/-}$ cells in a manner consistent with the T51B cells shown in Fig. 2.

Discussion

Phosphorylation of Cx43 appears to regulate the trafficking of Cx43 to the plasma membrane, assembly of Cx43 into gap junctional structures, single channel behavior and Cx43 degradation. The latter three events have been reported to be sensitive to TPA and, therefore, could be regulated by PKC (Kanemitsu and Lau, 1993; Lampe, 1994;
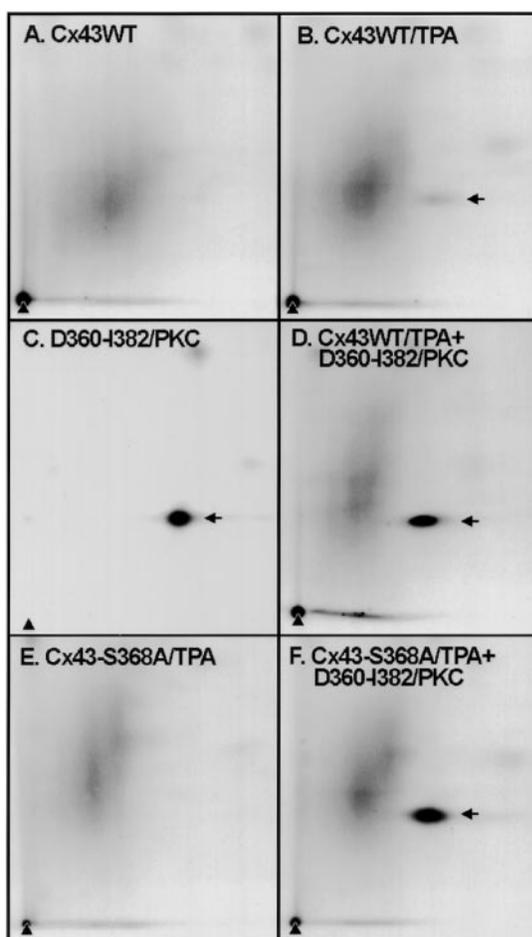

Figure 7. Two-dimensional phosphotryptic analysis of Cx43 derived from Cx43wt- and Cx43-S368A–transfected cells. Cx43 metabolically labeled and immunoprecipitated from Cx43$^{-/-}$ cells transfected with Cx43wt (22C-3 clone) either untreated (A) or treated (B) with TPA. (C) Peptide 360-382 of Cx43 phosphorylated by PKC. (D) Mixture of samples shown in B and C. (E) Cx43 metabolically labeled and immunoprecipitated from TPA-treated Cx43-S368A (22C-3 clone)–transfected Cx43$^{-/-}$ cells. F, Mixture of samples shown in C and E.

Kwak et al., 1995a,c). In this study, we demonstrate that phosphorylation of Cx43 on S368 is stimulated by TPA in vivo and mediated by PKC in vitro. Furthermore, electrophysiological studies of Cx43 and the Cx43-S368A mutant revealed that phosphorylation at S368 is necessary for a TPA-induced alteration of Cx43 channel behavior and contributes to decreased gap junctional communication.

Several laboratories have shown that Cx43 is phosphorylated on multiple serine and tyrosine residues (e.g., Figs. 4 A and 1 B). Mutation of some of these sites to nonphosphorylatable residues rendered cells expressing the mutant proteins insensitive to signaling cascades that would otherwise alter gap junctional communication (Swenson et al., 1990; Britz-Cunningham et al., 1995; Warn-Cramer et al., 1998; Zhou et al., 1999). L929 cells transfected with wild-type Cx43 or S364P-Cx43, showed an increase and no change, respectively, in Lucifer yellow dye transfer after microinjection of PKC and an increase and decrease, re-

spectively, after microinjection of cAMP-dependent protein kinase (Britz-Cunningham et al., 1995). These results suggest that the last 20 amino acids of Cx43 may contain multiple potential phosphorylation sites whose effects on intercellular communication can be altered by substitution of S364 with a proline residue and consequent changes in the secondary structure of this segment of the protein. In studies aimed at understanding the effects of phosphorylation on single channel behavior, Moreno et al. (1994) suggested that when Cx43 is phosphorylated (by unspecified kinases), the ~50- rather than ~100-pS conductance state is favored. Kwak et al. demonstrated that when either PKG (Kwak et al., 1995a,b) or PKC (Kwak et al., 1995a,c) is activated, a lower conductance state of the Cx43 channel is favored. In this study, a comparable change in the behavior of Cx43wt but not Cx43-S368A mutant channels was observed following activation of PKC with TPA. This result strongly suggests that phosphorylation at S368 in the COOH terminus of Cx43 is required for this change in channel behavior.

The observed increase in relative frequency of the ~50-pS event population and the concomitant loss of the ~100-pS population induced by TPA in Cx43wt-expressing cells could involve changes in channel number, unitary conductance or open probabilities. In view of the demonstrated inhibitory effects of PKC on channel assembly (Lampe, 1994) and the observed decrease in dye coupling in this and many other studies (e.g., Kanemitsu and Lau, 1993), it is unlikely that assembly and insertion of new channels is enhanced following TPA treatment of these cells. Thus, the increased relative frequency of the ~50-pS population could reflect: (a) conversion of the ~100-pS event population to ~50 pS (a unitary conductance change) or (b) a reduction in the open probability of the ~100-pS conductance state (to near zero) with enhanced open probability of the ~50-pS state.

Discriminating between changes in unitary conductance and open probability requires long, stable records of only one or two active channels which, given the long open and close times of these channels, were essentially nonexistent in this study. However, several observations suggest that phosphorylation induces a change in the unitary behavior of the channel. First, under control conditions ~50-pS transitions were entirely absent in several records. Similarly, ~100-pS events were entirely absent in several TPA records. Second, under both control and TPA conditions, 50- and 100-pS events were observed opening from and closing to the zero current level. Third, under control conditions when only one ~100-pS channel was active, closures to long-lived subconductance states of 50 pS were not observed. These observations suggest that Cx43 can assume two stable conductance states as was originally concluded by Moreno et al. (1994), and that the lower conductance state is favored by phosphorylation of S368. This conclusion is attractive but must be tempered by the lack of rigorous proof that normal channel behavior might include a 50-pS subconductance state whose open probability is increased by phosphorylation, a possibility that cannot be evaluated in our records due to the presence of halothane in all single channel experiments.

Activation of PKC in some cell types causes an increase in junctional conductance (Kwak et al., 1995c), whereas in other cell types it causes a decrease (Brissette et al., 1991; Berthoud et al., 1992, 1993; Reynhout et al., 1992; Lampe, 1994) or no change (Spray and Burt, 1990). Even in the same cell type, neonatal rat cardiomyocytes, all three responses to TPA have been reported: a decrease in junctional conductance (Munster and Weingart, 1993), an increase in junctional conductance (Kwak et al., 1995c) and little change in junctional conductance (Spray and Burt, 1990). The reasons for these differences within and particularly between cell types are not clear. It has been suggested that the variable response to TPA stems from differences: (a) inherent to cell lines vs. differentiated cells (Chanson et al., 1988; Munster and Weingart, 1993), (b) in the connexin's phosphorylation state before TPA exposure (Saez et al., 1997), (c) in the PKC isotypes expressed by the cells (Munster and Weingart, 1993), or (d) in experimental conditions (Munster and Weingart, 1993; Kwak et al., 1995c). Nevertheless, it is interesting to note that in an experiment where junctional conductance increased, the lower conductance state of the channel was still favored and dye coupling was still reduced following TPA treatment (Kwak et al., 1995c). Those data suggest that in addition to regulating the channel's conductance state (and consequently permeability), PKC activation can lead to changes in other parameters.

There are multiple mechanisms available to cells to regulate junctional conductance (including cell–cell adhesion, gap junction assembly, single channel behavior, and degradation). PKC or a TPA-induced kinase cascade may phosphorylate Cx43 at additional sites (compare Fig. 2, A–C) that affect these other mechanisms. For example, the S368A mutation appeared to have no effect on the TPA-mediated inhibition of gap junction assembly (data not shown). Decreased cell–cell adhesion or gap junction assembly could explain why the mutant clones (pI8 and pI9) showed different percentages of injections that resulted in no transfer in response to TPA. Since neither mutant clone showed an increase in frequency of the lower conductance state in response to TPA and the cells remaining coupled were coupled to a comparable degree, a separate PKC-mediated effect on gap junctions appears likely. It is interesting to note the presence of some 50-pS events in the Cx43-S368A–transfected cells. If the only site capable of producing this conductance level were S368, we would have expected this population of event amplitudes to be absent in the mutant transfected cells. Thus, other kinases may phosphorylate Cx43 at different sites and give rise to channels with comparable event amplitudes.

We would expect that at least one phosphorylation event on S368 must occur within each hexameric channel that is affected by TPA treatment. Indeed, the majority of Cx43 may be phosphorylated on S368 since Cx43 has a reduced mobility in SDS-PAGE after TPA treatment of T51B cells. However, the phosphorylation events that cause different shifts in mobility are unknown and our preliminary results indicate that cells containing S368A can still shift to some extent in response to TPA, so no definitive conclusions can be drawn at this time. We also do not know the kinetics of phosphorylation at S368 nor the cellular location of phosphorylation, although immunofluorescence labeling of the connexin in both cell types indicates that significant levels of Cx43 and Cx43-S368A

remain at the cell surface when the transfectants were similarly treated with TPA (data not shown). Comparison of the time course of the mobility shift in SDS-PAGE and the decreases in dye transfer (Kanemitsu and Lau, 1993) suggest that at least some PKC-mediated phosphorylation events occur before export to the plasma membrane (Lampe, 1994). Therefore, at least some phosphorylation at S368 might occur before gap junction assembly.

Phosphorylation of Cx43 at S368 was previously reported by Saez et al. (1997). They treated a fusion protein of glutathione-*S*-transferase and residues 243-382 of Cx43 with PKC in vitro and found that serines 368 and 372 were phosphorylated. However, these sites were not phosphorylated after treatment of rat cardiomyocytes with TPA in the presence of staurosporine, a potent kinase inhibitor, despite partial restoration of the staurosporine-induced decrease in junctional conductance. These results are difficult to compare with the current results due to different cell types, the prevalence of the lower conductance state of Cx43 in the rat cardiomyocytes in the absence of TPA stimulation (Burt and Spray, 1988), the presence of a potent kinase inhibitor, and the treatment conditions.

The phosphorylation and functional data presented here, together, strongly suggest that PKC directly phosphorylates Cx43 on S368, enhancing the relative frequency of a reduced conductance state and decreasing the relative frequency of the full open state. Using TPA as the effector, this study mechanistically connects changes in gap junctional channel properties with phosphorylation at a specific residue within Cx43. This series of observations reveals that phosphorylation at a single connexin site is sufficient to alter the behavior of gap junction channels and underscores the importance of this site as a mechanism for modifying junctional communication.

The results reported here with TPA-induced changes in junctional communication may also have broader significance in the area of carcinogenesis. An examination of more than two hundred known and potential carcinogens revealed that the ability of these molecules to promote carcinogenesis correlated better with their ability to inhibit intercellular communication than with their mutagenic potential (Rosenkranz et al., 1997). It remains to be seen how many of these agents affect channel behavior and how many alter other aspects of gap junction activity, such as assembly and turnover. Clarifying these effects will further our understanding of tumor promotion, carcinogenesis and the role of gap junctions in the control of cell growth.

References

Atkinson, M.M., A.S. Menko, R.G. Johnson, J.R. Sheppard, and J.D. Sheridan. 1981. Rapid and reversible reduction of junctional permeability in cells infected with a temperature-sensitive mutant of avian sarcoma virus. *J. Cell Biol.* 91:573–578.

Azarnia, R., and W.R. Loewenstein. 1984. Intercellular communication and control of cell growth. X. Alteration of junctional permeability by the *src* gene. *J. Membr. Biol.* 82:191–205.

Bazzi, M.D., and G.L. Nelsestuen. 1987. Association of protein kinase C with phospholipid vesicles. *Biochemistry.* 26:115–122.

Bazzi, M.D., and G.L. Nelsestuen. 1992. Autophosphorylation of protein kinase C may require a high order of protein-phospholipid aggregates. *J. Biol. Chem.* 267:22891–22896.

Berthoud, V.M., M.L.S. Ledbetter, E.L. Hertzberg, and J.C. Saez. 1992. Connexin43 in MDCK cells: regulation by a tumor-promoting phorbol ester and calcium. *Eur. J. Cell Biol.* 57:40–50.

Berthoud, V.M., M. Rook, E.L. Hertzberg, and J.C. Saez. 1993. On the mechanism of cell uncoupling induced by a tumor promoter phorbol ester in cloned 9 cells, a rat liver epithelial cell line. *Eur. J. Cell Biol.* 62:384–396.

Beyer, E.C., D.L. Paul, and D.A. Goodenough. 1987. Connexin43: a protein from rat heart homologous to a gap junction protein from liver. *J. Cell Biol.* 105:2621–2629.

Brissette, J.L., N.M. Kumar, N.B. Gilula, and G.P. Dotto. 1991. The tumor promoter 12-*O*-tetradecanoylphorbol-13-acetate and the *ras* oncogene modulate expression and phosphorylation of gap junction proteins. *Mol. Cell. Biol.* 11:5364–5371.

Britz-Cunningham, S.H., M.M. Shah, C.W. Zuppan, and W.H. Fletcher. 1995. Mutations of the connexin43 gap junction gene in patients with heart malformations and defects of laterality. *New Engl. J. Med.* 332:1323–1329.

Burt, J.M., and D.C. Spray. 1988. Single-channel events and gating behavior of the cardiac gap junction channel. *Proc. Natl. Acad. Sci. USA.* 85:3431–3434.

Burt, J.M., and D.C. Spray. 1989. Volatile anesthetics block intercellular communication between neonatal rat myocardial cells. *Circ. Res.* 65:829–837.

Chanson, M., R. Bruzzone, D.C. Spray, R. Regazzi, and P. Meda. 1988. Cell uncoupling and protein kinase C: correlation in a cell line but not in a differentiated tissue. *Am. J. Physiol.* 255:C699–C704.

Cooper, C.D., J.L. Solan, M.K. Dolejsi, and P.D. Lampe. 2000. Analysis of connexin phosphorylation sites. *Methods.* 20:196–204.

Crow, D.S., E.C. Beyer, D.L. Paul, S.S. Kobe, and A.F. Lau. 1990. Phosphorylation of connexin43 gap junction protein in uninfected and Rous sarcoma virus-transformed mammalian fibroblasts. *Mol. Cell. Biol.* 10:1754–1763.

de Feijter, A.W., J.S. Ray, C.M. Weghorst, J.E. Klaunig, J.I. Goodman, C.C. Chang, R.J. Ruch, and J.E. Trosko. 1990. Infection of rat liver epithelial cells with c-Ha-*ras*: correlation between oncogene expression, gap junctional communication and tumorigenicity. *Mol. Carcinog.* 3:54–67.

Dunham, B., S. Liu, S. Taffet, E. Trabka-Janik, M. Delmar, R. Petryshyn, S. Zheng, and M. Vallano. 1992. Immunolocalization and expression of functional and nonfunctional cell-to-cell channels from wild-type and mutant rat heart connexin43 cDNA. *Circ. Res.* 70:1233–1243.

Fishman, G.I., A.P. Moreno, D.C. Spray, and L.A. Leinwand. 1991. Functional analysis of human cardiac gap junction channel mutants. *Proc. Natl. Acad. Sci. USA.* 88:3525–3529.

Fitzgerald, D.J., and H. Yamasaki. 1990. Tumor promotion: models and assay systems. *Tetragen. Carcinog. Mutagen.* 10:89–102.

Goodenough, D.A., J.A. Goliger, and D.L. Paul. 1996. Connexins, connexons, and intercellular communication. *Annu. Rev. Biochem.* 65:475–502.

Hannun, A.C., C.R. Loomis, and R.M. Bell. 1985. Activation of protein kinase C by Triton X-100 mixed micelles containing diacylglycerol and phosphatidylserine. *J. Biol. Chem.* 260:10039–10043.

He, D.S., J.X. Jiang, S.M. Taffet, and J.M. Burt. 1999. Formation of heteromeric gap junction channels by connexins 40 and 43 in vascular smooth muscle cells. *Proc. Nat. Acad. Sci. USA.* 96:6495–6500.

Kadle, R., J.T. Zhang, and B.J. Nicholson. 1991. Tissue-specific distribution of differentially phosphorylated forms of Cx43. *Mol. Cell. Biol.* 11:363–369.

Kamps, M.P., and B.M. Sefton. 1989. Acid and base hydrolysis of phosphoproteins bound to Immobilon facilitates analysis of phosphoamino acids in gel-fractionated proteins. *Anal. Biochem.* 176:22–27.

Kanemitsu, M.Y., and A.F. Lau. 1993. Epidermal growth factor stimulates the disruption of gap junctional communication and connexin43 phosphorylation independent of 12-O-tetradecanoyl 13-acetate-sensitive protein kinase C: the possible involvement of mitogen-activated protein kinase. *Mol. Biol. Cell.* 4:837–848.

Kwak, B.R., M.M.P. Hermans, H.R. De Jonge, S.M. Lohmann, H.J. Jongsma, and M. Chanson. 1995a. Differential regulation of distinct types of gap junction channels by similar phosphorylating conditions. *Mol. Biol. Cell.* 6:1707–1719.

Kwak, B.R., J.C. Saez, R. Wilders, M. Chanson, G.I. Fishman, E.L. Hertzberg, D.C. Spray, and H.J. Jongsma. 1995b. Effects of cGMP-dependent phosphorylation on rat and human connexin43 gap junction channels. *Pflugers Arch. Eur. J. Physiol.* 430:770–778.

Kwak, B.R., T.A.B. Van Veen, L.J.S. Analbers, and H.J. Jongsma. 1995c. TPA increases conductance but decreases permeability in neonatal rat cardiomyocyte gap junction channels. *Exper. Cell Res.* 220:456–463.

Laemmli, U.K. 1970. Cleavage of structural proteins during the assembly of the head of bacteriophage T4. *Nature.* 227:680–685.

Laird, D.W., K.L. Puranam, and J.P. Revel. 1991. Turnover and phosphorylation dynamics of connexin43 gap junction protein in cultured cardiac myocytes. *Biochem. J.* 273:67–72.

Laird, D.W., P. Fistouris, G. Batist, L. Alpert, H.T. Huynh, G.D. Carystinos,

and M.A. Alaoui-Jamali. 1999. Deficiency of connexin43 gap junctions is an independent marker for breast tumors. *Cancer Res.* 59:4104–4110.

Lampe, P.D. 1994. Analyzing phorbol ester effects on gap junction communication: a dramatic inhibition of assembly. *J. Cell Biol.* 127:1895–1905.

Loo, L.W.M., J.M. Berestecky, M.Y. Kanemitsu, and A.F. Lau. 1995. pp60src-mediated phosphorylation of connexin 43, a gap junction protein. *J. Biol. Chem.* 270:12751–12761.

Martyn, K.D., W.E. Kurata, B.J. Warn-Cramer, J.M. Burt, E. TenBroek, and A.F. Lau. 1997. Immortalized connexin43 knockout cell lines display a subset of biological properties associated with the transformed phenotype. *Cell Growth Diff.* 8:1015–1027.

Moennikes, O., A. Buchmann, T. Ott, K. Willecke, and M. Schwarz. 1999. The effect of connexin32 null mutation on hepatocarcinogenesis in different mouse strains. *Carcinogenesis.* 20:1379–1382.

Moreno, A.P., J.C. Saez, G.I. Fishman, and D.C. Spray. 1994. Human connexin43 gap junction channels. Regulation of unitary conductances by phosphorylation. *Circ. Res.* 74:1050–1057.

Munster, P.N., and R. Weingart. 1993. Effects of phorbol ester on gap junctions of neonatal rat heart cells. *Pflugers Archiv. Eur. J. Physiol.* 423:181–188.

Musil, L.S., E.C. Beyer, and D.A. Goodenough. 1990. Expression of the gap junction protein connexin43 in embryonic chick lens: Molecular cloning, ultrastructural localization, and post-translational phosphorylation. *J. Membrane Biol.* 116:163–175.

Nishizuka, Y. 1986. Studies and perspectives of protein kinase C. *Science.* 233:305–312.

Ramanan, S.V., and P.R. Brink. 1993. Multichannel recordings from membranes which contain gap junctions. II. Substates and conductance shifts. *Biophys. J.* 65:1387–1395.

Reynhout, J.K., P.D. Lampe, and R.G. Johnson. 1992. An activator of protein kinase C inhibits gap junction communication between cultured bovine lens cells. *Exp. Cell Res.* 198:337–342.

Rosenkranz, M., H.S. Rosenkranz, and G. Klopman. 1997. Intercellular communication, tumor promotion and non-genotoxic carcinogenesis: relationships based on structural considerations. *Mutation Res.* 381:171–188.

Russo, G.L., M.T. Vandenberg, I.J. Yu, Y.-S. Bae, B.R. Franza, Jr., and D.R. Marshak. 1992. Casein kinase II phosphorylates p34cdc2 kinase in G1 phase of HeLa cell division cycle. *J. Biol. Chem.* 267:20317–20325.

Saez, J.C., A.C. Nairn, A.J. Czernik, G.I. Fishman, D.C. Spray, and E.L. Hertzberg. 1997. Phosphorylation of connexin43 and the regulation of neonatal rat cardiac myocyte gap junctions. *J. Mol. Cell Cardiol.* 29:2131–2145.

Shannon, J.D., and J.W. Fox. 1995. Identification of phosphorylation sites by Edman degradation. *Tech. Protein Chem.* VI:117–123.

Simon, A.M., D.A. Goodenough, E. Li, and D.L. Paul. 1997. Female infertility in mice lacking connexin37. *Nature.* 385:525–529.

Simon, A.M., D.A. Goodenough, and D.L. Paul. 1998. Mice lacking connexin40 have cardiac conduction abnormalities characteristic of atrioventricular block and bundle branch block. *Curr. Biol.* 8:295–298.

Spray, D.C., and J.M. Burt. 1990. Structure-activity relationships of the cardiac gap junction channel. *Am. J. Physiol.* 258:C195–C205.

Stagg, R.B., and W.H. Fletcher. 1990. The hormone-induced regulation of contact-dependent cell-cell communication by phosphorylation. *Endocr. Rev.* 11:302–325.

Sullivan, S., and T.W. Wong. 1991. A manual method for identification of phosphorylated amino acids in phosphopeptides. *Anal. Biochem.* 197:65–68.

Swenson, K.I., H. Piwnica-Worms, H. McNamee, and D.L. Paul. 1990. Tyrosine phosphorylation of the gap junction protein connexin43 is required for pp60src-induced inhibition of communication. *Cell Regul.* 1:989–1002.

Temme, A., A. Buchman, H.C. Babriel, E. Nelles, M. Scharz, and K. Willecke. 1997. High incidence of spontaneous and chemically-induced liver tumors in mice deficient for connexin 32. *Curr. Biol.* 7:713–718.

Trosko, J.E., C.C. Chang, B.V. Madhukar, and J.E. Klaunig. 1990. Chemical, oncogene, and growth factor inhibition of gap junctional intercellular communication: an integrative hypothesis of carcinogenesis. *Pathobiol.* 58:265–278.

Valiunas, V., R. Weigart, and P.R. Brink. 2000. Formation of heterotypic gap junction channels by connexins 40 and 43. *Circ. Res.* 86:E42–E49.

Warn-Cramer, B.J., G.T. Cottrell, J.M. Burt, and A.F. Lau. 1998. Regulation of connexin-43 gap junctional intercellular communication by mitogen-activated protein kinase. *J. Biol. Chem.* 273:9188–9196.

Zhou, L., E.M. Kasperek, and B.J. Nicholson. 1999. Dissection of the molecular basis of pp60(v-src) induced gating of connexin 43 gap junction channels. *J. Cell Biol.* 144:1033–1045.